ANALYSIS OF THE CONTROL BEHAVIOR OF A BIDIRECTIONAL HIGH-FREQUENCY DC-DC-CONVERTER

Johann W. KOLAR, Felix A. HIMMELSTOSS and Franz C. ZACH

Technical University of Vienna - Power Electronics Section
Gusshausstrasse 27-29, A - 1040 Vienna, AUSTRIA

ABSTRACT

A new system for DC-DC power conversion based on a boost converter topology is presented which makes power flow in both directions possible. The possibility of bidirectional power flow will increase the system dynamics and is also useful for certain applications, such as uninterruptable power supplies (UPS) etc. The structure is compared with the well known unidirectional boost converter. Open loop control is treated based on simulation using duty cycle averaging. The validity of the duty cycle averaging is proven by comparison to a switching model. The system behavior of the bidirectional converter is analyzed; a structure diagram is given.

1. INTRODUCTION

Unidirectional converters in their basic configuration are characterized by an asymmetrical structure regarding their topology and/or regarding their controllability. Switching instants and conduction intervals of the diodes on the secondary are - dependent on the converter topology (buck or boost converters etc.) - determined indirectly by changing the switching status of the power transistor on the primary.

An intrinsic limitation of this concept is given by the direction of current and energy flow (first quadrant of the current-voltage phase plane) which is determined by the direction of the electric valves.

Bidirectional power flow between constant voltage (current) sources requires replacement of the unidirectional power semiconductor devices by an antiparallel combination of a directly (power transistor) and an indirectly (diode) controllable electrical valve. This results in a unidirectionally controllable power semiconducter. However, this requires fixed voltage polarity, equivalent to restriction to the first and second quadrant of the current-voltage plane.

The application of this general concept to a boost converter structure leads to a topology with a remarkably simple topology.

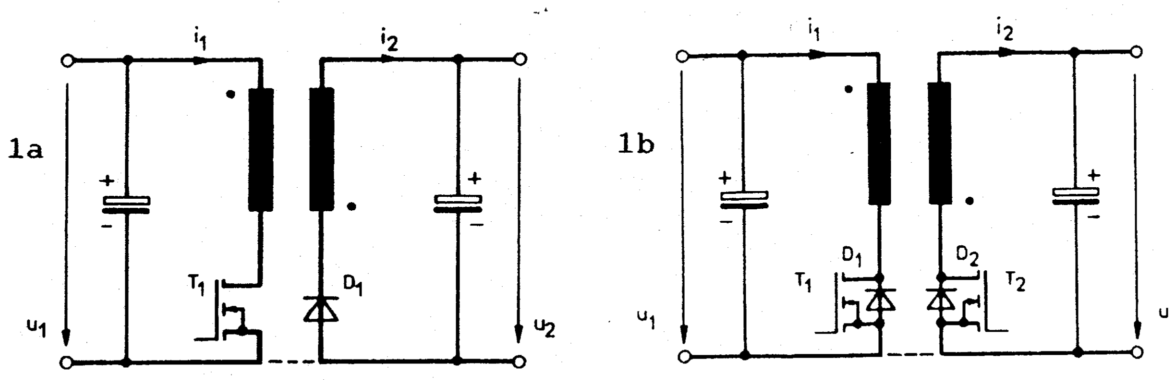

Fig.1 a) unidirectional boost converter
b) bidirectional boost converter

There is only one magnetic device necessary; see Fig.1 where this topology is compared to that of the conventional unidirectional boost converter.

The stationary system condition is characterized by a time constant average energy content of the primary and secondary electrical and magnetic energy storage devices. This equilibrium between energy input and output corresponds to a duty ratio defined only by the voltage ratios (and turn ratios) of primary and secondary independent of the energy flow direction. This is shown in the following. Idealized components are assumed and the push-pull control of T_1 and T_2 as indicated in Fig.2.

Vice versa by giving a duty ratio (for stationary, i.e. equilibrium operation) the voltage ratio of the converter can be varied to a large extent.

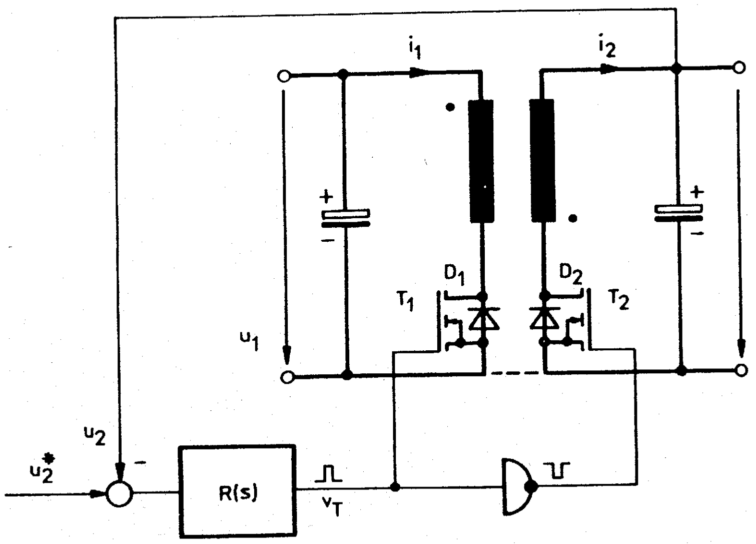

Fig.2 Bidirectional converter with push-pull control

2. SYSTEM DESCRIPTION AND COMPARISON OF UNIDIRECTIONAL AND BIDIRECTIONAL BOOST CONVERTER

Conventional boost converters are characterized by their continuous and discontinuous operation dependent on the load condition (and dimensioning) based on their unidirectional structure. This characterization takes place besides their basic function and the limitation to a defined energy flow direction (diode D_2 in Fig.2).

Discontinuous operation is given as shown in Fig.3 if the energy contents of the magnetic storage device is going to zero within the conduction intervall of D_2, i.e. before the power transistor T_1 is turned on again. In the following current free pause neither the diode (which suppresses the current reversal) nor the power transistor (which is not turned on) conduct.

Continious operation is given if the transistor on the primary is turned on again before i_{D2} reaches zero (Fig.3).

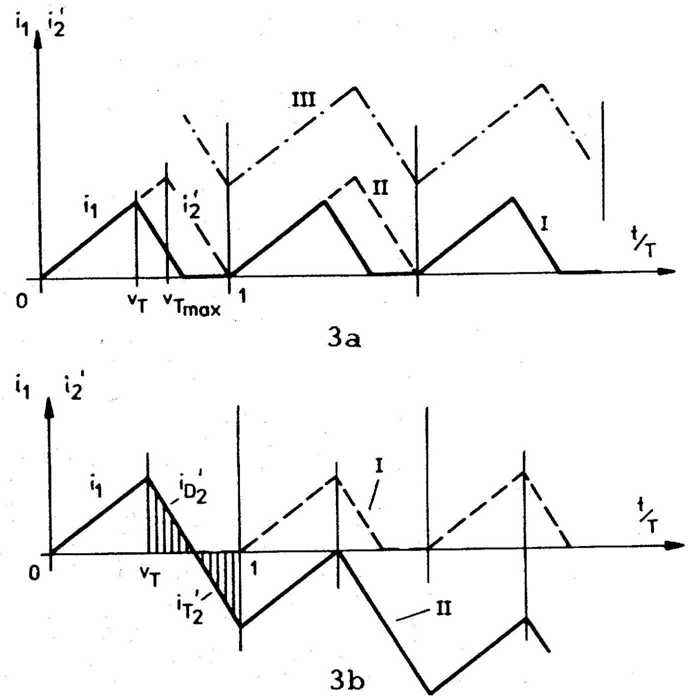

Fig.3

a) Unidirectional converter
- I : discontinuous current
- II : intermediate case
- III: continuous current

b) Bidirectional converter
- I : discontinuous current (usually not used for bidirectional operation)
- II: continuous mode

One area of interest (concerning dimensioning of the transformer, stress on power semiconductors etc.) would be the possibility of optimization via choice of the operating mode; this shall not be persued here, however, for the sake of brevity. Another area of interest lies especially in the control of the converter since the system structure changes (regarding order of the system, stationary gain etc.) when transition between continuous and discontinuous operation takes place. This is especially important because this transition in connection with simple basical control methods possibly can significantly deteriorate the control dynamics of the closed loop and possibly can lead to instability. This would require a limitation of the operating region.

If (as shown in Fig.2) the transistor T_2 controlled in a push-pull mode with respect to T_1 is situated antiparallel to D_2, the system remains in continuous operation independent of the load condition.

An intervall with zero current is suppressed by conduction of T_2 when i_2 passes through zero. Due to D_1 being antiparallel to T_1 it is evident that the primary current is not limited to positive values. This can be seen from the symmetry of the circuit since primary and secondary side basically are interchangeable. This also results in the possibility of reversing the energy flow. The system shows the behavior dependent on the load condition which corresponds to the continuous operating mode of a conventional boost converter. For the no load condition the current (related to the primary) oscillates around zero due to the primary and secondary current mean values then becoming zero. This is exactly valid for the loss free case. This is equivalent to the energy oscillation between input and output according to the switching frequency.

If one considers a practical realization of the circuit (where a discussion of realization with bipolar transistors is not persued here) one has to note that T_2 (T_1) conducts part of the current besides D_2 (D_1); this is due to the gate signal (push-pull control) being present also for positive i_2 (negative i_1); the current distribution corresponds to the parallel circuit of turn-on resistance and nonlinear diode characteristic.

Since low voltage MOSFETs have very low R_{DSon} (some 10 mΩ) the current almost exclusively is conducted by the FET. This naturally also leads to low conduction losses. A further advantage of controlling (gating) the switch is given by avoiding the considerable reduction of the maximum allowable value of du/dt of the transistor (base diffusion current due to the minority carriers); this appears after the conduction of the internal inverse diode (collector-base diode of the parasitic bipolar transistor). One more advantage is given by avoiding the high reverse current peak typical for the blocking behavior of the integrated diode. Only for high inverse currents in the pentode working region of the FET and due to the positive temperature coefficient of the turn-on resistance the diode characteristic will largely determine the behavior.

High voltage FETs show higher on-resistances (in the order of magnitude of 1 Ω) due to the on-resistance increasing with the power of 2.5 dependent on the blocking voltage. A modification of the antiparallel diode characteristic therefore is only given for the lower current region. In connection with the previous remarks it seems advantageous therefore to block the internal inverse diode by a Schottky diode in series and to add a fast diode externally.

In general the continuous operation given here establishes high requirements concerning turn-off behavior of the diodes D_1 and D_2. This obviously makes proper selection of the relevant power semiconductors especially important.

Concerning efficiency of the described system one has to note critically that, as mentioned, for no (low) load condition the energy oscillates between input and output. This leads to a considerable deterioration of the efficiency in connection with the nonideal behavior of the system components. The resistive losses appearing thereby can be reduced by reduction of the current ripple (increase of the effective inductances, increased size and volume, stray inductances). Further losses are due to magnetizing and demagnetizing the transformer core with switching frequency, which is largely load independent, however. This appears for each turn off as energy converted into heat being proportional to the sum of the stray inductances and the square of the current ripple maximum; thereby one also has to consider that the blocking voltage across the semiconductor switch is formed by the sum of supply voltage plus the transformed secondary voltage plus the voltage across the stray inductance.

On the other hand there are no limitations concerning dimensioning of the transformer core as compared to unidirectional concepts where the dimensioning has to take place under consideration of a chosen operational mode for all load conditions. This offers an additional degree of freedom for optimizing the system behavior.

An efficiency improvement for low output load is possible by proper system control besides proper dimensioning of the system. Such a control is based on maintaining of discontinuous operation of the conventional unidirectional converter (T_1 and D_1 are conducting, Fig.1a).

When energy reversal is required T_1 is blocked and only T_2 is controlled (T_2, D_1 are conducting). A sporadic reversal of energy flow basically can not take place due to D_1 and D_2. Losses due to energy oscillations are avoided; for no load condition in the ideal case neither T_1 nor T_2 are triggered (Fig.1b or 2).

If no galvanic separation is required between primary and secondary, the structure is simplified according to Fig.4. It resembles the topology of one phase leg of a pulse width modulated converter whose DC link capacitor is divided into C_1 and C_2 and whose base is connected via the storage inductance to the capacitive voltage center.

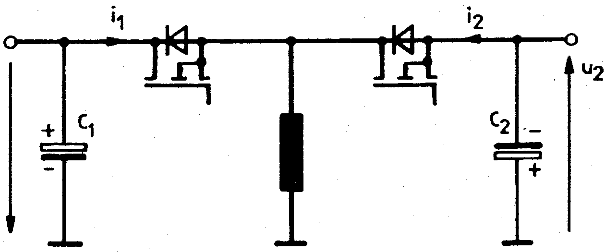

Fig.4 Nonisolated bidirectional converter structure

The expression for the voltage transformation ratio for push-pull operation and transformer coupling employs also the turns ratio (besides the duty ratio). Therefore this gives an additional dergee of freedom for dimensioning in order to avoid extreme duty ratios; this therefore could be used even if in a simple version galvanic seperation would not be required. Application of a transformer also brings the advantage that the output voltage polarity can be selected such that the negative end of input and output voltages have common ground.

It is obviously advantageous for galvanic coupling of input and output circuits to realize power switch T_1 as n-FET and switch T_2 as p-FET (or vice versa) and to use a common driver stage. Of course, one has to consider limitations of p-FET technology.

Due to direct coupling of the gate capacitances and (negative) feedback of the drain voltage rise via the drain-gate (Miller) capacitance on the gate voltage behavior and due to the requirement of inverse polarity of gate voltages for T_1 and T_2 for turn-on, simultaneous conduction of both transistors would lead to a short circuit of the input and output circuits, limited only by lead inductances.

Delay between turn-on of one and turn-off of the other transistor poses no problem. This is contrary to an overlap which has to be avoided by all means. This is because if synchronism ("synchronous rectification function") is neglected there is always possible a current commutation from a transistor (primary or secondary) to a diode (secondary or primary) and vice versa, but not directly from transistor to transistor. This in all cases makes formation possible of a primary or secondary current corresponding to the magnetization status of the transformer.

Concerning control of the system the following concepts or combinations thereof are thinkable, dependent on the special application and operation (continuous or discontinuous). (Thereby we would like to limit the considerations to constant switching frequency.)

- Fixed input and output voltages:
  Energy exchange is definable by current control.

- Fixed input voltage:
  Control of the output voltage (produced by the converter system) via the duty ratio (pulse width modulation) of the power switches.

- Fixed output voltage:
  Input voltage produced by the converter system, principle as before.

As an example we want to mention the application of the concept described here for a realization of an uninterruptable power supply (charging and decharging of a battery). This power supply is realized for discontinuous operation such as in [1]; the control of the battery voltage u_2 will be switched over to input (load) voltage control for a mains failure. Therefore, due to the bidirectionality of the structure, one can achieve a considerably lower realization effort as compared to an antiparallel arrangement of two unidirectional converters.

In the following we want to treat exclusively the concept of the bidirectional continuous boost converter (with constant switching frequency) because the discontinuous mode is basically not different from that of the simple unidirectional system.

3. MODEL REPRESENTATION OF THE BIDIRECTIONAL CONVERTER

In the following there is an outline of the derivation of the model equations for the bidirectional converter.

3.1 Complete Model (Including Parasitic Elements)

Parasitic elements considered are the (ohmic) resistances on the primary and secondary R_1, R_2 (consisting of the sums of the winding resistances and the R_{DSon} of the semiconductor switches) and the equivalent series resistance (ESR) of the output capacitor. During the interval t_{on} the equivalent circuit of Fig.5a is valid, leading to the equations

$$\frac{d(u_C)}{dt} = - \frac{u_C}{C \cdot (R+ESR)} , \tag{1}$$

$$\frac{d(\Phi)}{dt} = \frac{u_1}{N_1} - \frac{R_1}{L_1} \cdot \Phi . \tag{2}$$

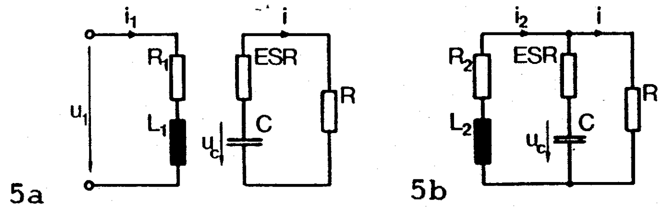

Fig.5 Equivalent circuit of the converter
a) turn-on switching state
b) turn-off switching state

During the interval t_{off} the equivalent circuit of Fig.5b is applicable; the corresponding equations are

$$\frac{d(u_C)}{dt} = -\frac{u_C}{C\cdot(R+ESR)} + \frac{R}{C\cdot(R+ESR)}\cdot\frac{N_2\cdot\Phi}{L_2} \quad , \tag{3}$$

$$\frac{d(\Phi)}{dt} = -\frac{u_C}{N_2}\cdot\frac{R}{R+ESR} - \Phi\cdot\frac{R_2\cdot(R\|ESR)}{L_2} \quad . \tag{4}$$

These two sets of equations therefore describe the system behavior. Under the condition that the system time constants are large compared to the switching period we can combine these two sets of equations. The duty ratio shall be defined as

$$\alpha = V_T = \frac{t_{on}}{T} \quad . \tag{5}$$

Weighted by this duty ratio, the combination of the two sets yields

$$\frac{d(u_C)}{dt} = -\frac{u_C}{C\cdot(R+ESR)} + (1-\alpha)\cdot\frac{R}{R+ESR}\cdot\frac{N_2}{C\cdot L_2}\cdot\Phi \quad , \tag{6}$$

$$\frac{d(\Phi)}{dt} = -(1-\alpha)\cdot\frac{u_C}{N_2}\cdot\frac{R}{R+ESR} - \Phi\cdot\left[\frac{R_1}{L_1}\cdot\alpha + (1-\alpha)\cdot\frac{R_2+R\|ESR}{L_2}\right] + \alpha\cdot\frac{u_1}{N_1} \quad . \tag{7}$$

3.2 System linearization of the complete model

The set of equations is transformed into a linearized system around the operating point by introducing

$$
\begin{aligned}
u &= u_o + \hat{u} \quad , \\
u_c &= u_{co} + \hat{u}_c \quad , \\
\Phi &= \Phi_o + \hat{\Phi} \quad , \\
\alpha &= \alpha_o + \hat{\alpha} \quad , \\
u_1 &= u_{1o} + \hat{u}_1 \quad .
\end{aligned}
\tag{8}
$$

This results in the following equations

$$
\frac{d(\hat{u}_c)}{dt} = -\frac{1}{C\cdot(R+ESR)}\cdot\hat{u}_c + \frac{R\cdot N_2}{C\cdot L_2\cdot(R+ESR)}\cdot(1-\alpha_o)\cdot\hat{\Phi} - \frac{R\cdot N_2\cdot\Phi_o}{C\cdot L_2\cdot(R+ESR)}\cdot\hat{\alpha} \quad , \tag{9}
$$

$$
\begin{aligned}
\frac{d(\hat{\Phi})}{dt} = &-\frac{R\cdot(1-\alpha_o)}{N_2\cdot(R+ESR)}\cdot\hat{u}_c - \\
&- \left[\alpha_o\cdot\frac{R_1}{L_1} + (1-\alpha_o)\cdot\frac{R_2+R_2\|ESR}{L_2}\right]\cdot\hat{\Phi} + \\
&+ \left[\frac{R}{R+ESR}\cdot\frac{u_{co}}{N_2} - \Phi_o\cdot\left[\frac{R_1}{L_1} - \frac{R_2+R_2\|ESR}{L_2}\right] + \frac{u_{1o}}{N_1}\right]\cdot\hat{\alpha} + \\
&+ \frac{\alpha_o}{N_1}\cdot\hat{u}_1 \quad ,
\end{aligned}
\tag{10}
$$

and

$$
\hat{u} = \hat{u}_c\cdot\frac{R}{R+ESR} + \hat{\Phi}\cdot(R\|ESR)\cdot(1-\alpha_o)\cdot\frac{N_2}{L_2} - \hat{\alpha}\cdot\Phi_o\cdot\frac{N_2}{L_2}\cdot(R\|ESR) \quad . \tag{11}
$$

With the further simplification ESR << R and R_2 >> ESR we arrive at the following state vector representation of the bidirectional converter:

$$\begin{bmatrix} \dfrac{d(\hat{u}_c)}{dt} \\ \dfrac{d(\hat{\Phi})}{dt} \end{bmatrix} = \begin{bmatrix} A_{11} & A_{12} \\ A_{21} & A_{22} \end{bmatrix} \cdot \begin{bmatrix} \hat{u}_c \\ \hat{\Phi} \end{bmatrix} + \begin{bmatrix} B_{11} \\ B_{21} \end{bmatrix} \cdot \hat{\alpha} + \begin{bmatrix} C_{11} \\ C_{21} \end{bmatrix} \cdot \hat{u}_1 \quad , \tag{12}$$

$$\hat{u} = \begin{bmatrix} D_{11} & D_{12} \end{bmatrix} \cdot \begin{bmatrix} \hat{u}_c \\ \hat{\Phi} \end{bmatrix} + d \cdot \hat{\alpha} \quad . \tag{13}$$

with

$$A_{11} = -\frac{1}{R_o \cdot C} \ , \qquad A_{12} = (1-\alpha_o) \cdot \frac{N_2}{C \cdot L_2} \ ,$$

$$A_{21} = -\frac{1-\alpha_o}{N_2} \ , \qquad A_{22} = -\left[\alpha_o \cdot \frac{R_1}{L_1} + (1-\alpha_o) \cdot \frac{R_2}{L_2} \right] \ ,$$

$$B_{11} = -\frac{\Phi_o \cdot N_2}{C \cdot L_2} \ , \qquad B_{21} = \frac{u_{1o}}{N_1} + \frac{u_{co}}{N_2} \ , \tag{14}$$

$$C_{11} = 0 \ , \qquad C_{21} = \frac{\alpha_o}{N_1} \ ,$$

$$D_{11} = 1 \ , \qquad D_{21} = ESR \cdot (1-\alpha_o) \cdot \frac{N_2}{L_2} \ ,$$

$$d = \Phi_o \cdot N_2 \cdot \frac{ESR}{L_2} \quad .$$

This leads to the following structure diagram Fig.6.

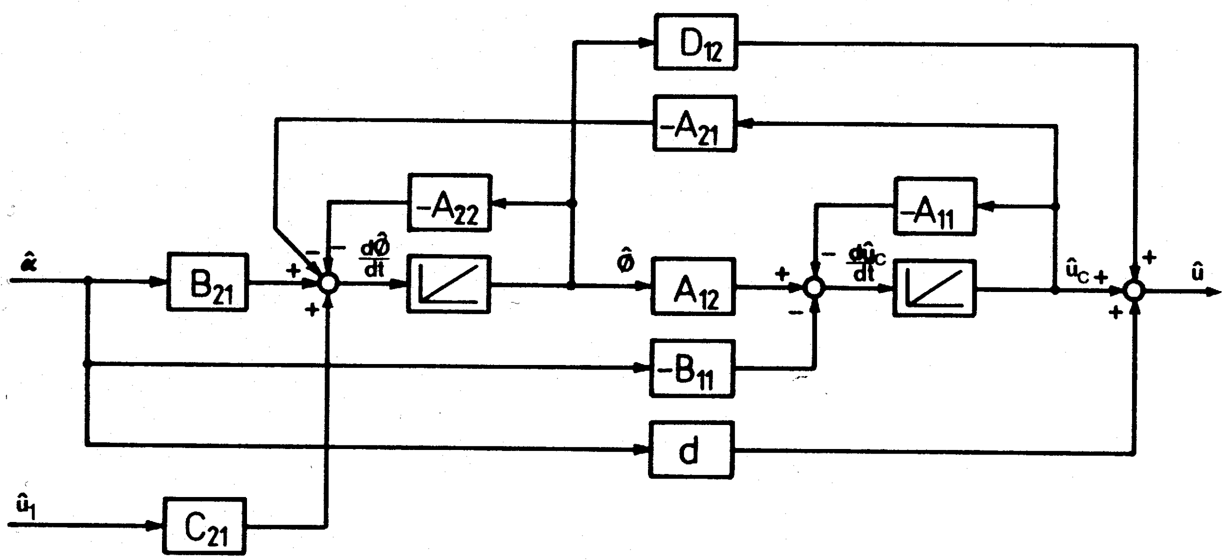

Fig.6 Structure diagram of the linearized bidirectional push-pull converter

3.3 Simple Model (Without Parasitic Elements)

In the following a model is outlined where the parasitic elements R_1, R_2 and ESR are neglected. The equations weighted by the duty ratio now are

$$\frac{d(u_c)}{dt} = (1-\alpha)\cdot\frac{\Phi\cdot N_2}{L_2\cdot C} - \frac{u_c}{R\cdot C} , \tag{15}$$

$$\frac{d(\Phi)}{dt} = \alpha\cdot\frac{u_1}{N_1} - (1-\alpha)\cdot\frac{u_c}{N_2} . \tag{16}$$

In the stationary case we have therefore

$$u_{co} = \frac{N_2}{N_1}\cdot\frac{\alpha_o}{1-\alpha_o}\cdot u_{1o} , \qquad \Phi_o = \frac{u_{co}}{R_o}\cdot\frac{L_2}{N_2\cdot(1-\alpha_o)} . \tag{17}$$

With a linearization method as previously used (Eqs.(8)) we receive a simple state space representation

$$
\begin{bmatrix} \dfrac{d(\hat{u}_c)}{dt} \\ \dfrac{d(\hat{\Phi})}{dt} \end{bmatrix} = \begin{bmatrix} A_{11} & A_{12} \\ A_{21} & A_{22} \end{bmatrix} \cdot \begin{bmatrix} \hat{u}_c \\ \hat{\Phi} \end{bmatrix} +
$$

$$
\begin{bmatrix} B_{11} \\ B_{21} \end{bmatrix} \cdot \hat{\alpha} + \begin{bmatrix} C_{11} \\ C_{21} \end{bmatrix} \cdot \hat{R} + \begin{bmatrix} D_{11} \\ D_{21} \end{bmatrix} \cdot \hat{u}_1 \quad , \qquad (18)
$$

with

$$
A_{11} = - \frac{1}{R_o \cdot C} \quad , \qquad A_{12} = (1-\alpha_o) \cdot \frac{N_2}{C \cdot L_2} \quad ,
$$

$$
A_{21} = - \frac{1-\alpha_o}{N_2} \quad , \qquad A_{22} = 0 \quad ,
$$

$$
B_{11} = - \frac{\Phi_o \cdot N_2}{C \cdot L_2} \quad , \qquad B_{21} = \frac{u_1}{N_1} + \frac{u_{co}}{N_2} \quad , \qquad (19)
$$

$$
C_{11} = \frac{u_{co}}{(R_o)^2 \cdot C} \quad , \qquad C_{21} = 0 \quad ,
$$

$$
D_{11} = 0 \quad , \qquad D_{21} = \frac{\alpha_o}{N_1} \quad .
$$

We now have a set of equations discribing the behavior of the system variables u_c (capacitor voltage, i.e. output voltage) and Φ (magnetic flux, i.e. basically current) for small changes of the duty ratio α, of the load resistance R and the input voltage u_1.

The transfer function of the system can be written as

$$
G(s) = k \cdot \frac{s - 1/T_1}{s^2 + 2 \cdot \delta \cdot \Omega_n + \Omega_n^2} \quad , \qquad (20)
$$

where k, T_1, δ and Ω_n would have to be determined from Eq.(18).

4. THE BIDIRECTIONAL CONVERTER WITH OPEN LOOP CONTROL

4.1 Large-Signal Behavior

Start-Up: Since for start-up there exists no counter-voltage on the secondary side yet, the transformer core is not demagnetized and the current rises continuously. For start-up a current limi-

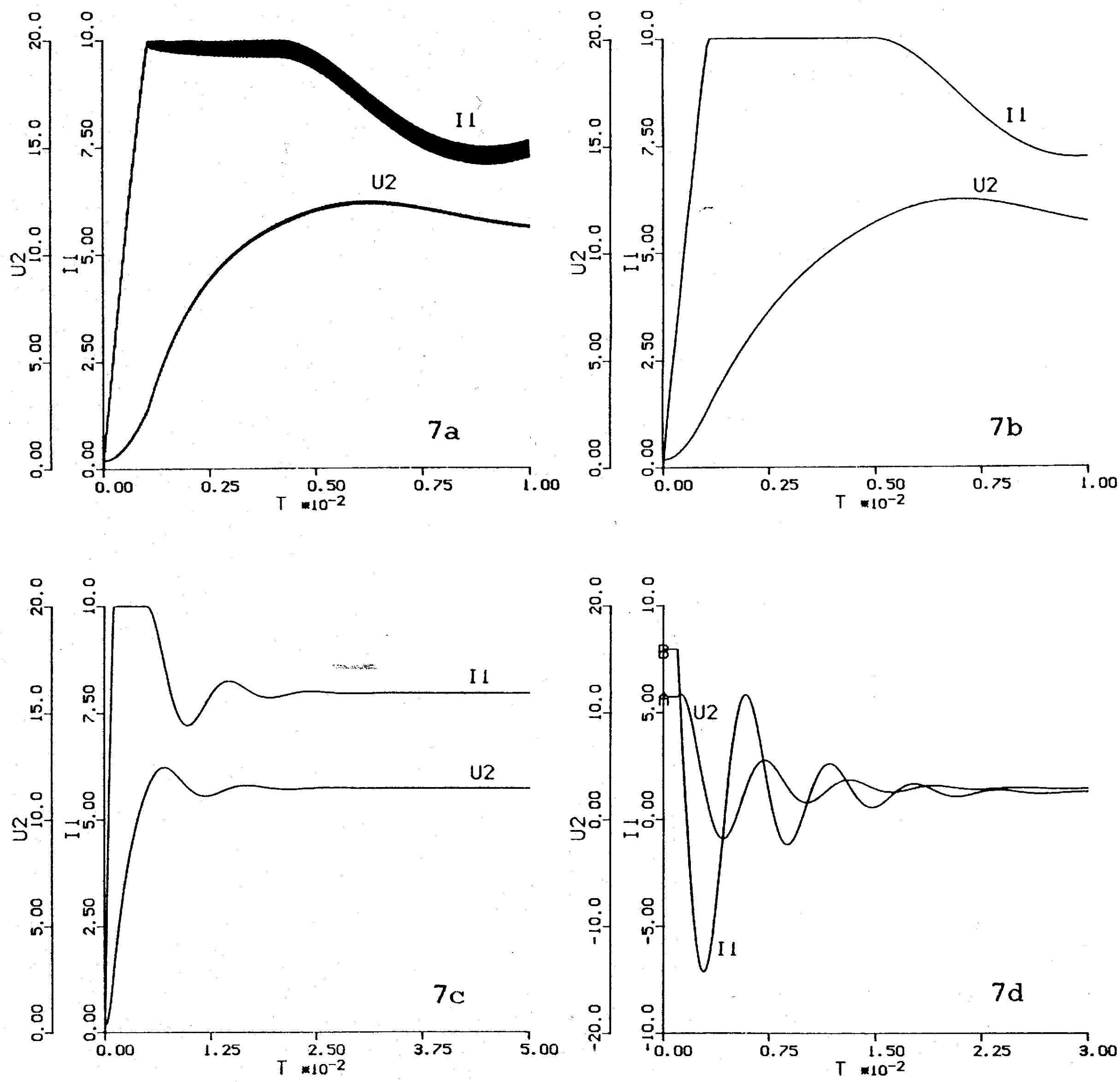

Fig.7 Large-signal behavior (axes in [V], [A] or [s])
a) start-up of the model converter
b) start-up of the model based on Eqs.(6) and (7)
c) as b) but calculated until the steady-state point
d) duty cycle step

tation is therefore necessary. Figure 7a shows the start-up of a model converter operating at 25 kHz switching frequency, where current limitation is applied. This is compared to the results of the calculation of the start-up where the Eqs.(6) and (7) are used with weighted duty ratios as mentioned. One can see the good consistancy of both results.

Duty Ratio Step: A duty ratio change leads to a change of the output voltage. From Fig.7d one can see the transient behavior being caused by a step of the duty ratio from 0.5 to 0.2. Also, a current reversal results. Furthermore, one can notice that the output voltage (which finally has to decrease) rises initially. This can be explained by the all-pass characteristic of the system.

4.2 Small Signal Behavior

In the following several selected system responses are shown. Due to the good system description by the Eqs.(6) and (7), as has been shown by a comparison of the results gained from this set and from Eqs. 1-4, one can use the former set. As a starting point an operation is chosen where $\alpha_o=0.5$ and where the load consumes 50 W with output voltage resulting from $\alpha_o=0.5$.

System response to a duty ratio step: Also in this case one can see the importance of current limitation; already a step of the duty ratio of 5% leads to such a high transient current that the current limitation has to interact. Even for this small duty ratio step one can notice the all-pass behavior of the system: the voltage rises or falls immediately after a decline or increase of the duty ratio (see the small notch in Fig.8a and Fig.8b).

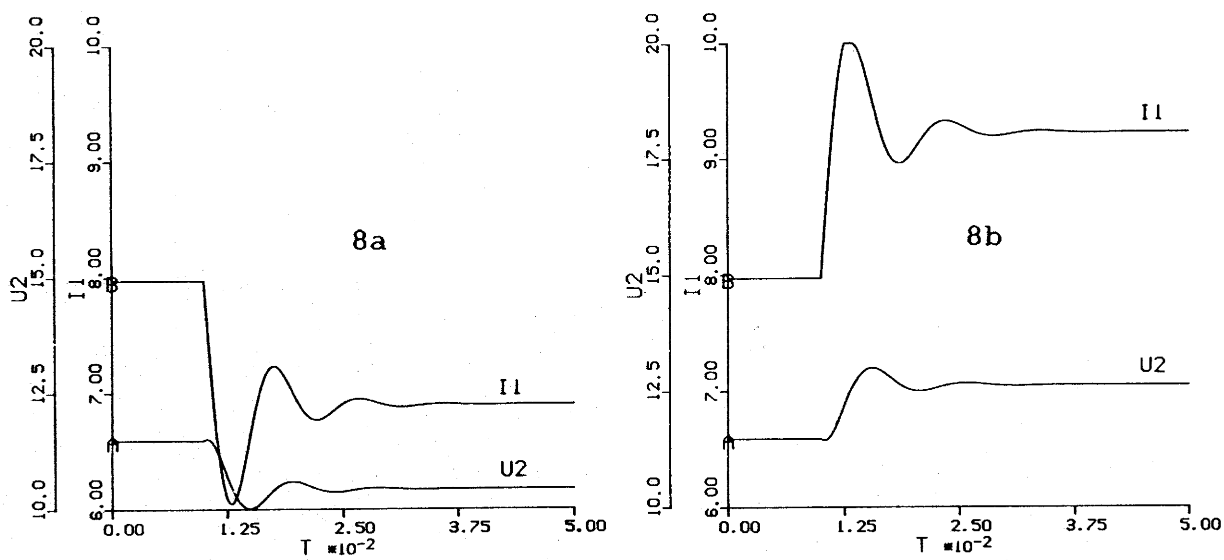

Fig.8 Duty cycle step response (U_2[V], I_1[A]) : a) -5%, b) +5%

System responds to a load step: The load step used here amounts to 1/10 of the output load (Fig.9).

System response to an input voltage step: The input voltage step for the shown system behavior (Fig.10) has a magnitude of 5%.

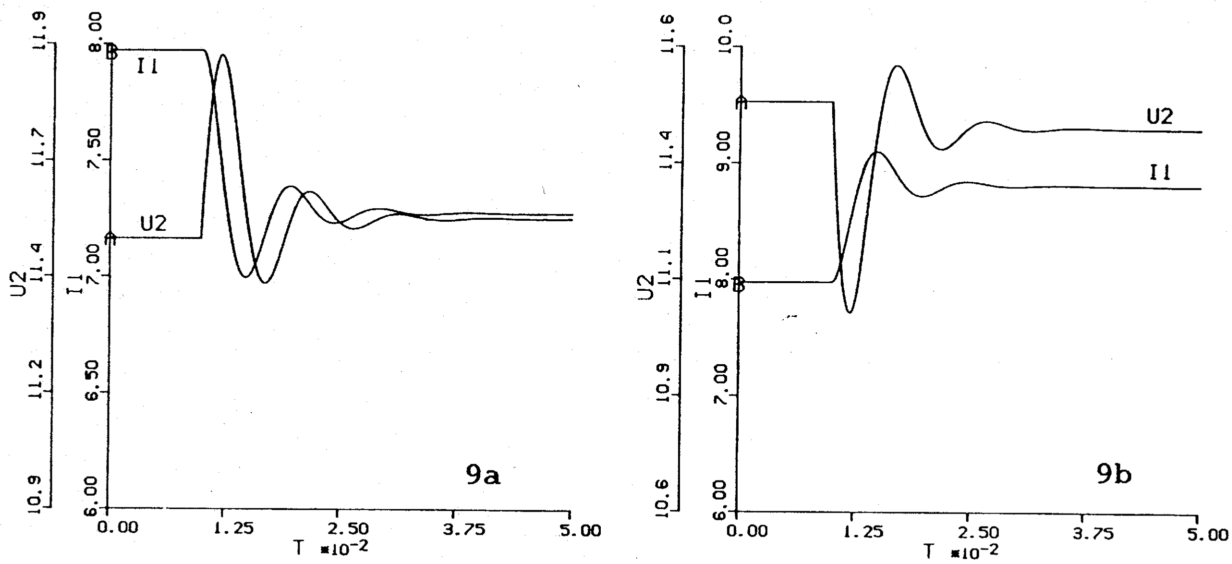

Fig.9 System response to a load step: a) -10%, b) +10%
(axes in [V], [A] or [s])

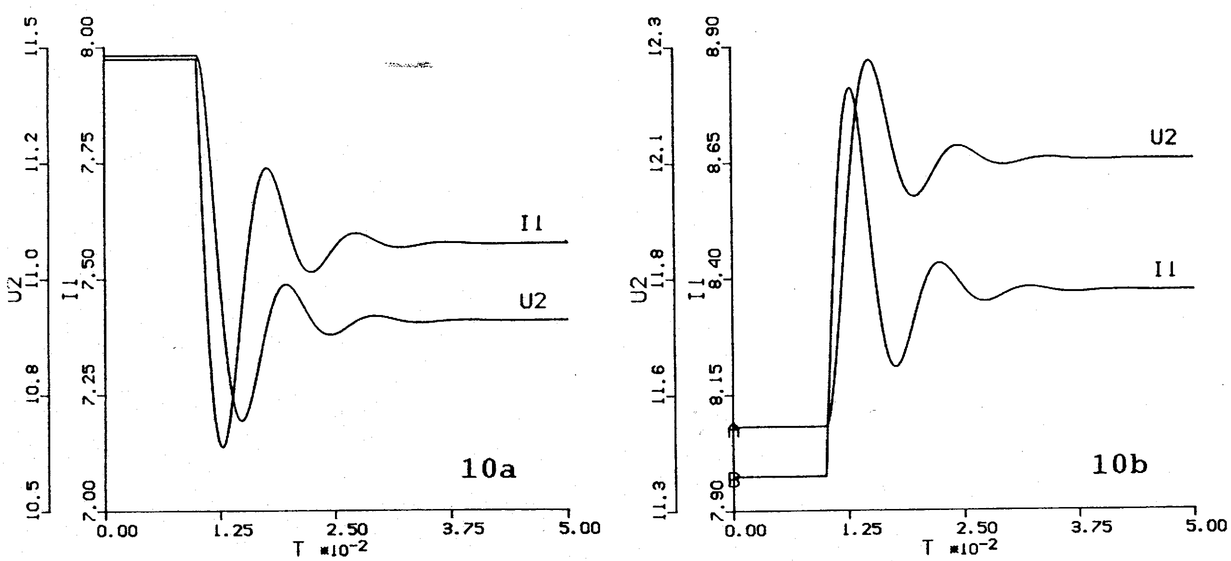

Fig.10 System response to an input voltage step
(axes in [V], [A] or [s]) : a) -5%, b) +5%

5. CONCLUSIONS

A new system for DC-DC power conversion based on a boost converter topology has been presented which makes power flow in both directions possible. This feature will increase the system dynamics and is also useful for certain applications, such as UPS. Open loop control has been treated based on simulation using duty cycle averaging. The advantage of this method is that the equations can be handled much more efficiently than the exact equations. The validity has been checked by comparison of the results of both sets of equations for characteristic cases.

As the research shows closed loop control will require application of controllers of higher sophistication, e.g. state space controllers, due to the all-pass character of the system. A further difficulty will be the nonlinearity of the system such that the system behavior varies according to the operating point. An optimized controller therefore should be adaptive. The relevant research is somewhat involved but shall be carried out in the near future.

REFERENCES

[1] WEINGARTEN, H.: «Ein im Zeitbereich arbeitendes automatisches Entwurfsverfahren für elektrische Filter», Archiv für Elektrotechnik, 62 (1980), Springer Verlag, pp.321-326.

ACKNOWLEDGEMENT

The authors are very much indebted to the Austrian «Fonds zur Förderung der wissenschaftlichen Forschung» who supports the work of the power electronics section at their university.